

FEM-DBEM procedure for crack analysis in baffle module of Wendelstein 7-X

R. Citarella¹, V. Giannella¹, M. Lepore¹, J. Fellingner²

¹Dept. of Industrial Engineering, University of Salerno

Via G. Paolo II, 132, 84084, Fisciano (SA), Italy

²Max-Planck-Institut Für Plasmaphysik

Teilinstitut Greifswald, Greifswald, Germany

rcitarella@unisa.it

Abstract: - “Wendelstein 7-X” is the world’s largest nuclear fusion experiment of “stellarator type” in which a hydrogen plasma is confined in a magnet field, generated with external superconducting coils, allowing the plasma to be heated up to fusion temperature. The water-cooled Plasma Facing Components (PFC) protect the Plasma Vessel (PV) against radiative and convective heat from the plasma.

After the manufacturing process of the heat shields and baffles, several cracks have been found in the braze and in the cooling pipes. Due to heat loads occurring during each Operational Phase (OP), thermal-stresses are generated in the heat sinks, brazes and cooling pipes, that encourage cyclic crack-growth and, eventually, the water leak through the pipes.

The aim of this study is to predict the operational limits of the baffles and heat shields under cyclic heat loads, by using a numerical model based on a FEM-DBEM approach, in order to provide an assessment on the risks of premature failure for segments assembled in the PV.

Key-Words: - FEM-DBEM approach; plasma vessel; plasma facing components; crack analysis

1 Introduction

Wendelstein 7-X (Fig. 1) [1], the world’s largest modular nuclear fusion experiment of stellarator type, is currently operating. A hydrogen plasma is confined in a magnet field generated with external superconducting coils that allow the plasma to be heated up to fusion temperatures without overheating the surrounding structure. The water cooled Plasma Facing Components (PFC) protect the Plasma Vessel (PV) against radiative and convective heat from the plasma. Depending on the expected heat loads, four types of PFC are basically used, see Fig. 2:

- highly loaded divertors, made of water cooled CuCrZr fingers, covered with carbon reinforced carbon tiles;
- moderately loaded heat shields;
- moderately loaded baffles, both made of CuCrZr heat sinks brazed on water cooled steel pipes and covered with bolted graphite tiles. The heat shields are flexibly supported with a few pins onto the PV

whereas the baffles are supported by rigid steel structures;

- lowly loaded wall panels, which consist of two parallel steel plates welded together and filled with cooling water.

High stresses develop in coils, superconducting cables [2] and supporting structure when the coils are charged, due to the EM Lorentz forces. In previous papers [3-4], several cracks, found in a Lateral Support Element (LSE) of the conducting coils of Wendelstein 7-X, were investigated using a coupled FEM-DBEM approach [5-9], in order to take advantage of the higher accuracy and flexibility of DBEM when handling three-dimensional crack growth simulations under mixed mode conditions [10-13]. Crack sizes and shapes, as well as stress states and SIFs along the crack front, were updated in each simulation step up to reaching a critical SIF value, corresponding to an unstable crack growth [14].

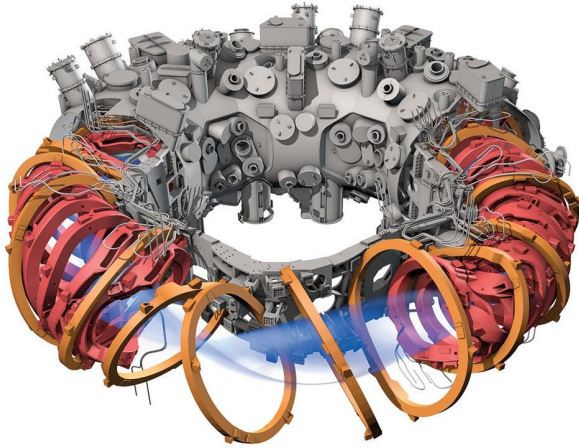


Fig. 1: Cut out view of Wendelstein 7-X.



Fig. 2: internal view of Plasma Vessel with basic types of Plasma Facing Components (PFCs).

Two different Operational Phases are basically designated for the Wendelstein 7-X; the first is represented by a load spectrum (Operational Phase 1 – OP1) consisting of different heat flux pulses applied on the graphite tiles, whereas, the second (Operational Phase 2 – OP2) is modelled by using a steady-state heat flux, again applied on the graphite tiles. In [15], different damage configurations for the same Baffle Module 7V were analysed considering the OP1 loading condition.

In this paper, several cracks discovered in the baffle modules of Wendelstein 7-X, are judged as potentially dangerous and consequently their propagation, when applying OP2 load spectrum, is simulated by using a FEM-DBEM numerical approach. The OP2 scheduled working conditions of W7-X are based on a steady-state heat flux applied on the graphite tiles for a total lapse of 6 mins. ABAQUS [16] and BEASY [17] commercial codes are adopted for FEM and DBEM analyses respectively.

2 Problem description

The heat shields and baffles are manufactured by brazing the heat sinks onto the cooling pipes and then bending the pipes in the desired form to match the shape of the PV. Afterwards, it has been found that, as a consequence of the pipe bending, needed to cope with the inner plasma vessel geometry (Fig. 1b), cracks appeared in the brazing and sometimes into the cooling pipes, at the terminal part of the brazed connection, causing partial detachment between braze and pipe (Fig. 3).

Due to heat loads occurring in each plasma pulse, thermal stresses are generated in the heat sinks, brazes and cooling pipes, which encourage cyclic crack-growths, with potential risks of cooling fluid leaks through the pipe (cracks growing into the pipe might cause a water leak that would interrupt operation of the machine and damage the surrounding structure).

The objective of this study is to predict the operational limits of the baffles and heat shields under cyclic heat loads under worst case assumption that cracks, as observed in the most damaged specimens, are present in the assembled structure. Notably, the worst cracks were observed in the baffle segments, as the corresponding cooling pipes were most strongly bent; consequently this study focuses on such segments.

A numerical procedure, based on the coupling of FEM and DBEM, was implemented to analyse the cracked zone and provide an assessment of fatigue failure risks for segments built in the PV.

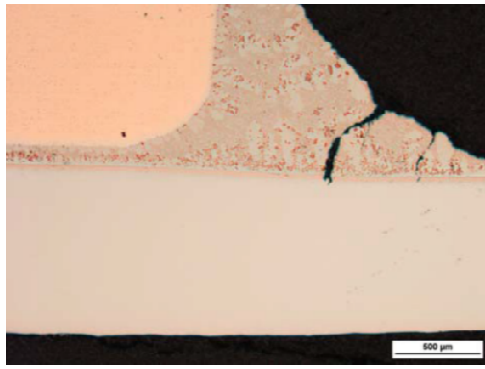
3 FEM analysis

3.1 FEM model

A FEM model involving the whole investigated Baffle Module BM-7V is produced (Fig. 4); it consists of CuCrZr heat sinks brazed on steel pipes and covered with graphite tiles, all supported with a rigid steel structure.

In this work, the OP2 load spectrum is considered, applying a steady-state heat flux, radiated on the graphite tiles, with a total magnitude equal to 100 kW/m² and a cooling pipe internal pressure equal to 25 bar.

The FE model comprises nearly 300.000 linear and quadratic elements.



(a)



(b)



(c)

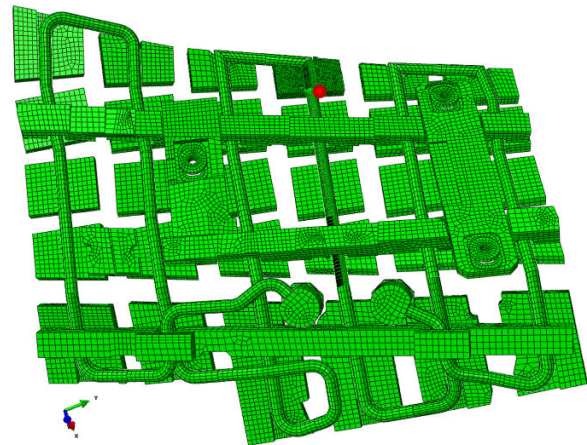


(d)

Fig. 3. Crack on components after manufacturing process: a) CT scan of a crack cutting through the braze and on the verge to start propagating in the pipe; b-d) external views of cracks in the braze.



(a)



(b)

Fig. 4. (a) Baffle Module 7V and (b) FEM model (the investigated zone is highlighted by a red dot).

The Finite Element Analysis (FEA) is split in two consecutive parts:

- a thermal FEA, in which the heat flux is applied on the graphite tiles in order to compute temperature and heat flux fields;
- a thermal-stress FEA, in which the previously calculated temperature field, in addition to the internal pipe pressure, are applied in order to assess the stress-strain fields.

An elastic-plastic constitutive model is adopted: in Tabs. 1-2, thermal and linear-elastic properties are listed.

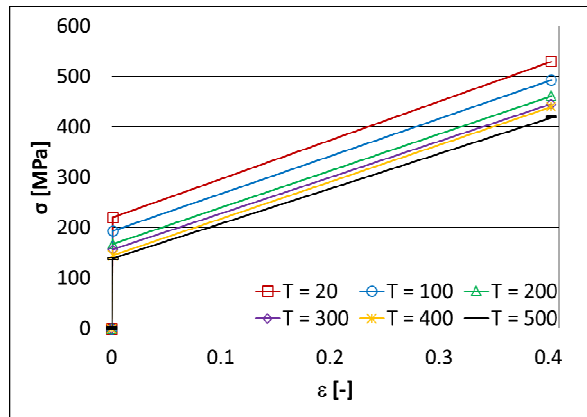
T [°C]	20	200	400	600	800
E [GPa]	200	184	168	152	126
α [1/°C]	1.59E-5	1.68E-5	1.78E-5	1.88E-5	-
K [kW/m/°C]	0.015	-	0.021	-	-
c_p [J/kg/°C]	472	-	520	-	-
ρ [kg/mm ³]	7.96E-6	-	-	-	-

Tab. 1. Material properties of SS 316L.

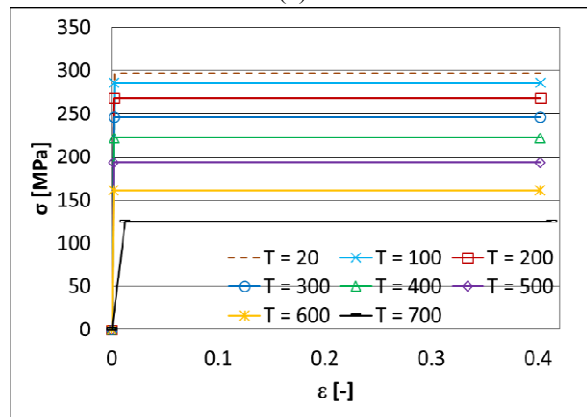
T [°C]	20	200	400	600	800
E [GPa]	130	120	110	95	10
α [1/°C]	1.59E-5	1.68E-5	1.78E-5	1.88E-5	-
K [kW/m/°C]	0.379	0.357	0.356	0.366	-
c_p [J/kg/°C]	388	-	-	473	-
ρ [kg/mm ³]	8.92E-6	-	-	-	-

Tab. 2. Material properties of CuCrZr.

Fig. 6 shows the adopted temperature-dependant elastic-plastic curves



(a)



(b)

Fig. 6. Temperature-dependant elastic-plastic constitutive laws for SS 316L (a) and CuCrZr (b).

3.2 FEM submodel

A FEM submodel (Fig. 7) is created in order to reduce dof's and speed up the interfacing with the DBEM code; moreover, refining the mesh in the crack surrounding zones, it is possible to assess with higher accuracy the stress solution, improving the accuracy of the crack growth prediction. The FEM submodel comprises nearly 36000 quadratic elements.

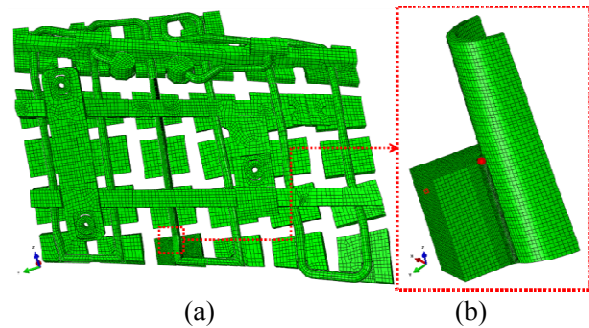
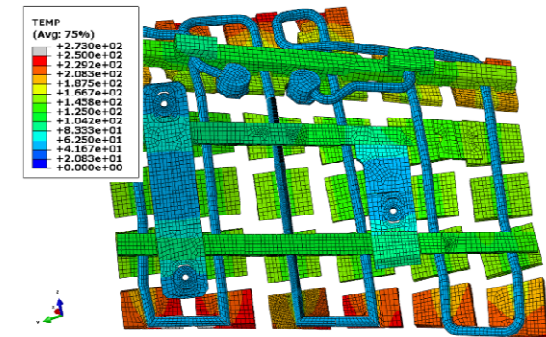


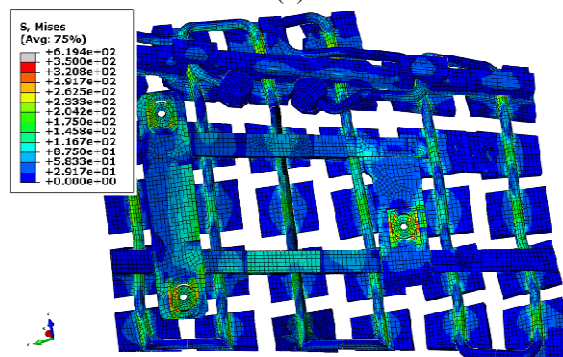
Fig. 7. a) FEM global model and b) FEM submodel (red dots to highlight crack insertion zone).

3.3 FEM results

A transient thermal FEA is applied to compute the temperature fields during the heat flux application phase. Then, a thermal-stress FEA computes the stress-strain field, using the previously calculated temperature distribution and the pipe internal pressure as boundary conditions. In Fig. 8, a temperature distribution and von Mises stress scenario are shown as obtained at the end of heat flux application (the instant causing the highest stresses is that immediately preceding the plasma switch off), as taken from OP2 load spectrum.



(a)



(b)

Fig. 8. (a) FEM temperature [°C] and (b) von Mises stress [MPa] field.

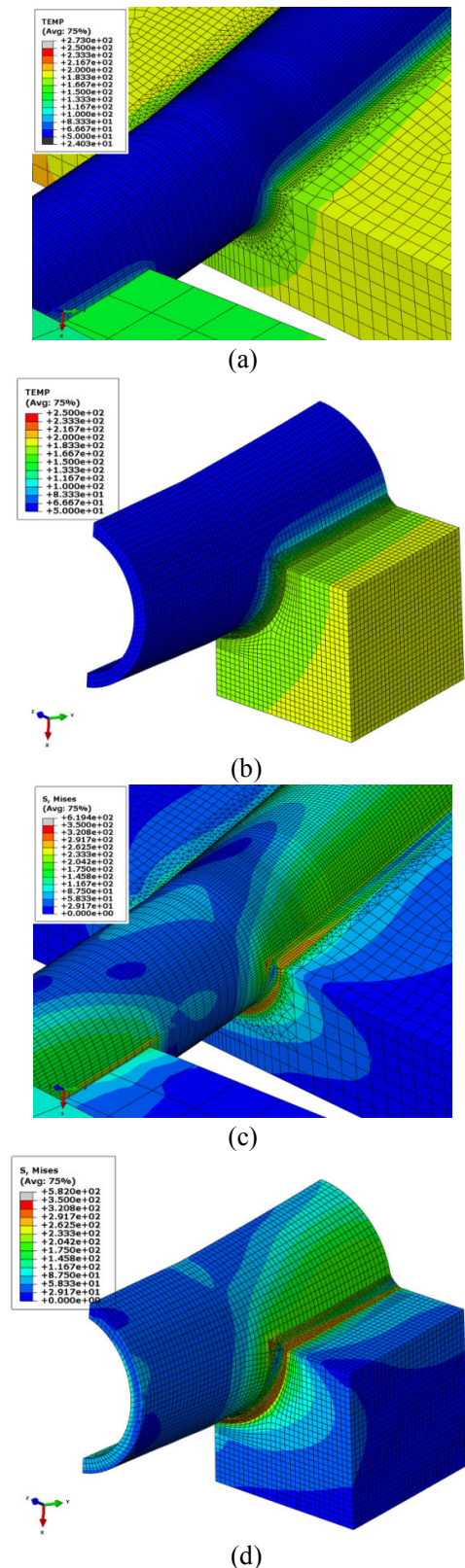


Fig. 9. Comparison between temperature fields [°C] of (a) FEM global model and (b) submodel, and between Von Mises stress fields [MPa] of (c) FE global model and (d) submodel.

Subsequently, FEM results from global model are used to define the boundary conditions for a FEM submodel. Such FEM submodel is solved and the matching between global and submodel results is verified for validation purpose (Fig. 9).

It is important to evidence a negligible yielding in correspondence of the submodel volume; this enables the possibility of a linear elastic analysis when analysing the fracture behaviour by DBEM.

4 DBEM analyses

4.1 DBEM submodel

A DBEM submodel is created (Fig. 10) applying a *skinning* procedure to the aforementioned FEM submodel; then it is solved under the hypothesis of linear elasticity and SIFs are evaluated for the investigated cracks.

Cracks were mostly observed in the brazed area of the baffle segments, as these cooling pipes were severely bent after the brazing process (Fig. 4), so it was necessary to explicitly model the braze bead in the DBEM model.

In order to simulate the crack propagation from the braze bead toward the pipe thickness, the merging of the two zones corresponding to braze and pipe in a single zone with homogeneous material properties was needed, because the adopted DBEM code cannot allow for a crack crossing two distinct zones. In particular, the thermal and mechanical properties of pipe material have been also attributed to the braze bead and no interface between pipe and braze bead has been modelled (Fig. 11). Clearly this merging between braze and pipe in one single zone introduces an element of approximation for the stress-strain solution in the affected volume, but this is judged acceptable because the target here is to get a first insight into the behaviour of a potential crack rather than providing a quantitative numerical-experimental correlation.

SIFs are evaluated using the J-integral approach [18, 19] and kink angles are assessed using the Minimum Strain Energy Density (MSED) [20] criterion.

A NASGRO crack growth law (Eq. 1) is adopted: it is calibrated at room temperature (even if, strictly speaking, the temperatures in the cracked area is nearly 100°C), by using the parameters related to SS 316L provided in NASGRO library (Tab. 3).

The boundary conditions applied on the DBEM submodel are the temperature and the displacement field provided by the FEM submodel analysis at the end of the heat flux application phase; in addition, a pressure equal to 2.5 MPa is applied on the pipe internal elements.

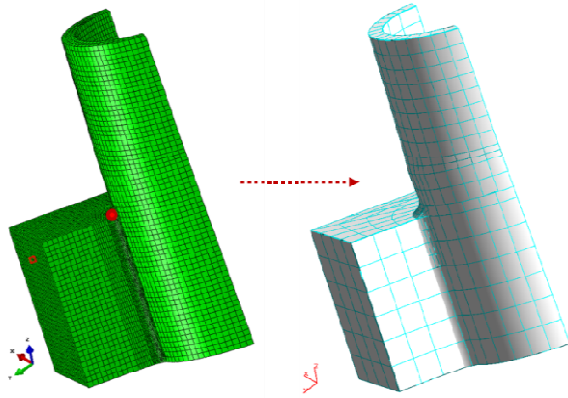


Fig. 10. DBEM submodel (red dots to highlight the crack insertion zones).

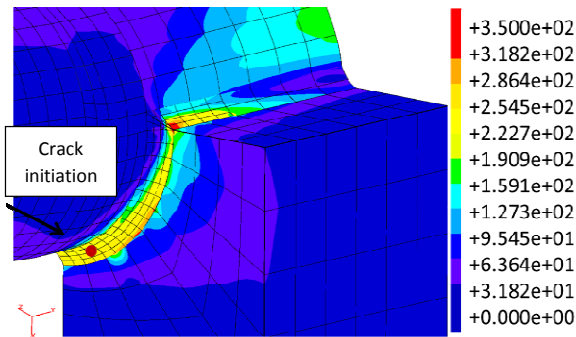


Fig. 11. Max Principal Stress [MPa] field showing the area in which to insert the crack

$$\frac{da}{dN} = \frac{C\Delta K^n \left(1 - \frac{\Delta K_{th}}{\Delta K}\right)^p}{\left(1 - \frac{\Delta K}{(1-R)K_C}\right)^q} \quad (1)$$

C	n	p	q	ΔK_C [MPa*mm ^{0.5}]	ΔK_{th} [MPa*mm ^{0.5}]
4.843E-13	3	0.25	0.25	6950	122

Tab. 3. SS 316L fracture properties at room temperature.

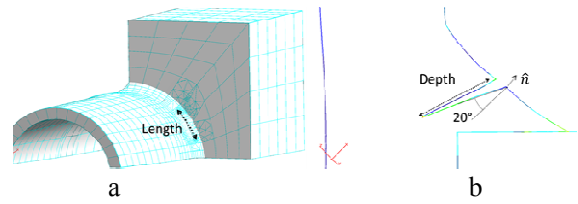


Fig. 12. Highlight of remeshed area and definition of crack sizes and orientation.

4.2 Crack configurations

Four crack configurations have been considered, as representative of the typology of cracks detected in the BM-7V components.

The modelled cracks differ each other for the initial crack size and orientation but have the same crack initiation point, chosen considering the zone of the submodel with the highest values of Max Principal Stress (Fig. 11).

The initial crack shape is semi-elliptical with variable sizes (Fig. 12) as listed in Tab. 4.

	Case 1	Case 2	Case 3	Case 4
Length [mm]	1.3	3	3.5	3
Depth [mm]	0.65	0.65	0.65	1

Tab. 4. Considered crack sizes.

4.3 DBEM results

The cracks to be analysed have been inserted at the selected crack insertion node of the uncracked DBEM model (Fig. 11), with consequent remeshing in the surrounding area (Fig. 12). Then, the stress-strain fields are recomputed for the DBEM cracked domains and eventually *J*-integrals are calculated at *J*-path positions along the crack front.

Figs. 13-16 show the DBEM cracked model with the related Max Principal Stress plots, whereas Fig. 17 shows the SIF variations along the crack fronts for the four considered cracks.

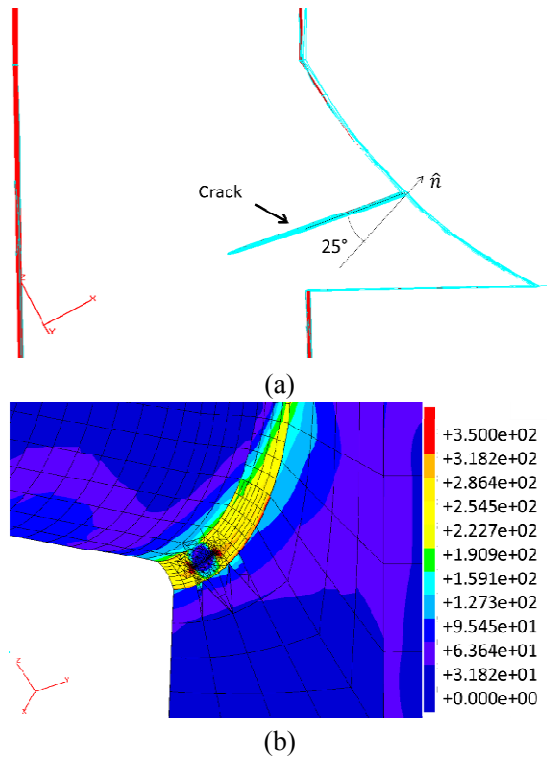


Fig. 13. Case 1: (a) Crack inserted into the DBEM model; (b) Max Principal Stress field [MPa] in the crack surroundings.

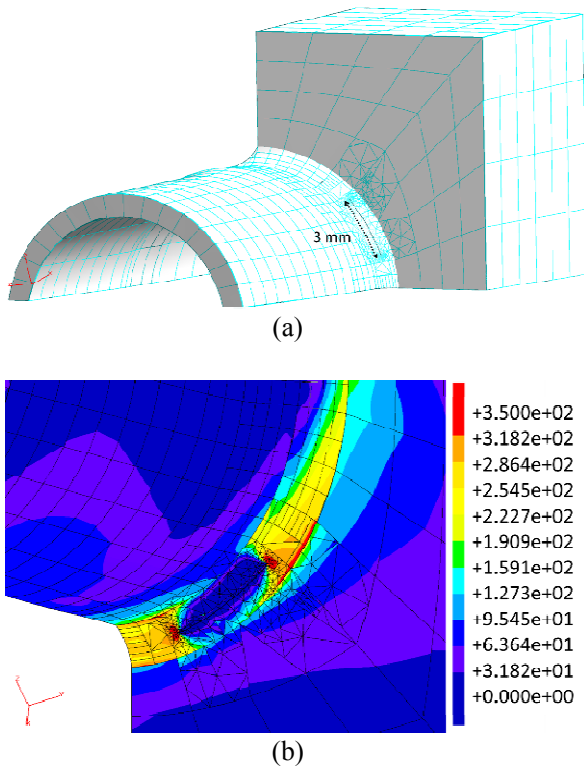


Fig. 14. Case 2: (a) Crack inserted into the DBEM model; (b) Max Principal Stress field [MPa] in the crack surroundings.

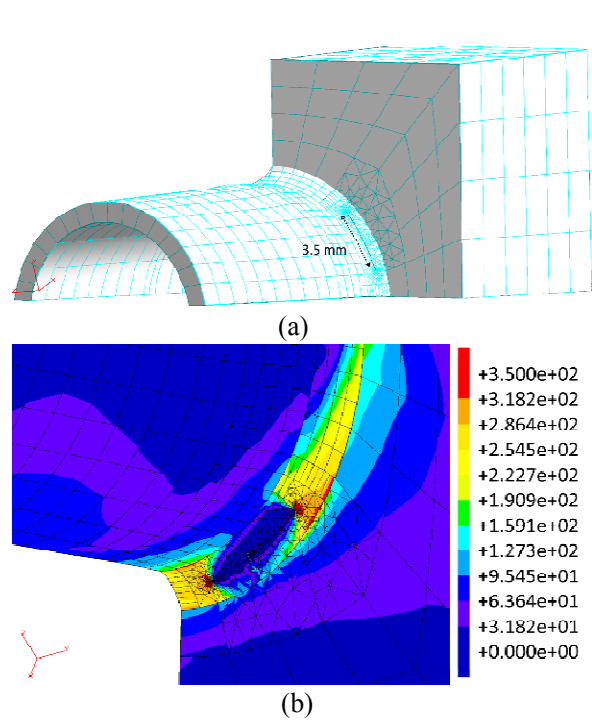


Fig. 15. Case 3: (a) Crack inserted into the DBEM model; (b) Max Principal Stress field [MPa] in the crack surroundings.

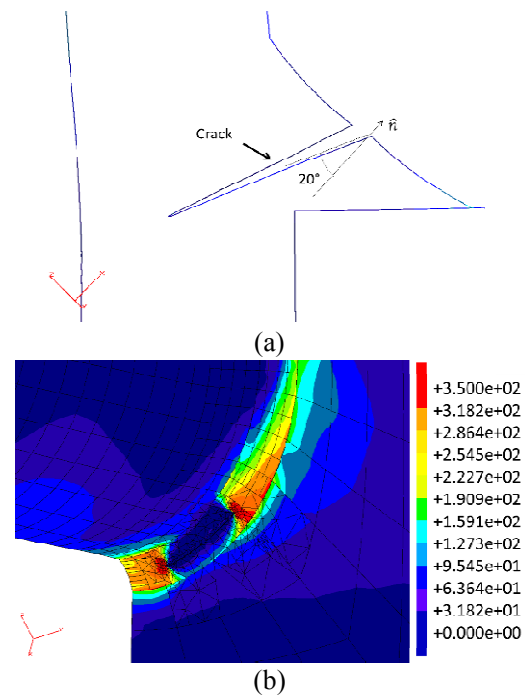
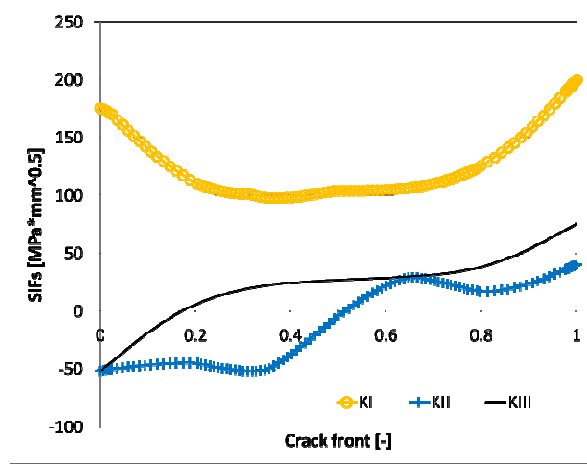
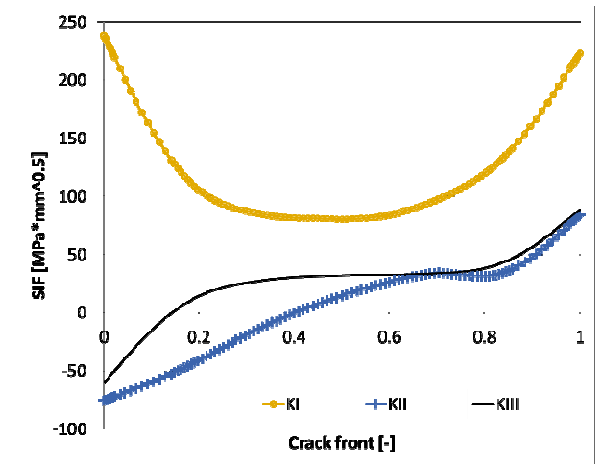


Fig. 16. Case 4: (a) Crack inserted into the DBEM model; (b) Max Principal Stress field [MPa] in the crack surroundings.

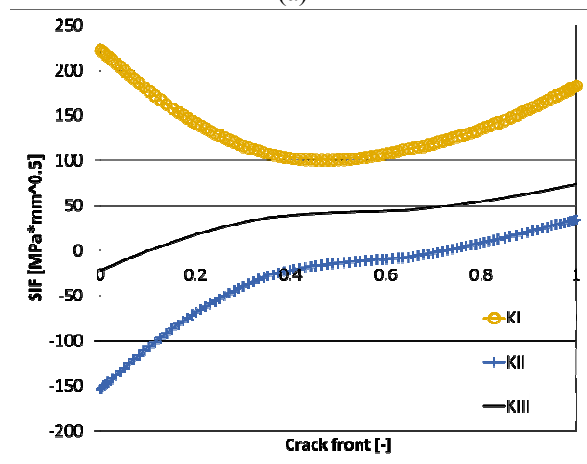


(a)

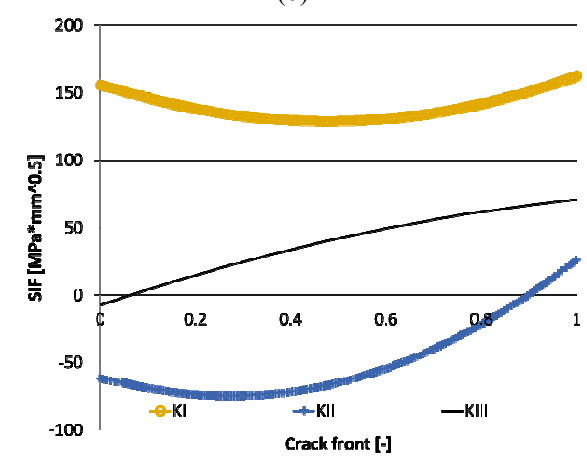


(d)

Fig. 17. SIFs distribution along the crack fronts for: (a) case 1, (b) case 2, (c) case 3, (d) case 4.



(b)



(c)

4.4 Discussion

Four different crack configurations have been proposed to simulate the crack typologies observed in the Baffle Module 7V of Wendelstein 7-X. In all cases the ΔK_{th} is exceeded along the crack front suggesting the need for a simulation of crack propagation in order to assess the load cycles before failure. Moreover the level of risk inherent with each scenario can be inferred by the relative values of SIFs along the crack front.

5 Conclusions

Several cracks have been introduced in the numerical model of a steel pipe brazed onto a CuCrZr heat sink, with the aim to assess the potential condition of water leakage due to cyclic crack growth through the pipe thickness.

The considered PFC is the Baffle Module 7V, undergoing a steady-state heat flux (Operational Phase 2 loading condition) and a cooling fluid pressure.

The adopted FEM-DBEM approach enables to simulate fracture problems by resorting to the advantages of FEM and DBEM methods: the FEM code is used to work out the main global thermal-stress analysis considering the loads applied on the entire component, whereas, the fracture analyses are completely demanded to the DBEM code.

In all the analysed crack configurations the ΔK_{th} is exceeded suggesting the need for a simulation of crack propagation in order to assess the load cycles

before failure. Further developments will see the simulation of a fatigue crack propagation for those scenarios considered most dangerous.

References

- [1] Bykov V., et al., Structural analysis of W7-X: Overview, *Fusion Engineering & Design*, Vol. 84, pp. 215–219, 2009.
- [2] Corato V., et al., *Detailed design of the large-bore 8T superconducting magnet for the NFASSY test facility*, Supercond. Sci. Technol., 28 (034005), 1-9, 2015.
- [3] Citarella R., Lepore M., Fellingner J., Bykov V., Schauer F., *Coupled FEM-DBEM method to assess crack growth in magnet system of Wendelstein 7-X*, *Frattura ed Integrità Strutturale* 26 92-103, 2013.
- [4] Citarella R., Lepore M., Perrella M., Fellingner J., *Coupled FEM-DBEM approach on multiple crack growth in cryogenic magnet system of nuclear fusion experiment 'Wendelstein 7-X'*, *Fatigue and Fracture of Engineering Material and Structures*, Vol. 39, pp. 1488–1502, 2016.
- [5] Citarella R., Cricri G., Lepore M., Perrella M., *Thermo-Mechanical Crack Propagation in Aircraft Engine Vane by Coupled FEM-DBEM Approach*, *Advances in Engineering Software*, Vol. 67, pp. 57-69, 2014.
- [6] Citarella R., Cricri G., *A two-parameter model for crack growth simulation by combined FEM-DBEM approach*, *Advances in Engineering Software*, Vol.40, No.5, pp. 363–377, 2009.
- [7] Citarella R., Carlone P., Lepore M., Sepe R., *Hybrid technique to assess the fatigue performance of multiple cracked FSW joints*, *Engineering Fracture Mechanics*.
- [8] Citarella R., Giannella V., Vivo E., Mazzeo M., *FEM-DBEM approach for crack propagation in a low pressure aeroengine turbine vane segment*, *Theoretical and Applied Fracture Mechanics*, doi:10.1016/j.tafmec.2016.05.004.
- [9] Carlone P., Citarella R., Lepore M., Palazzo G.S., *A FEM-DBEM investigation of the influence of process parameters on crack growth in aluminium friction stir welded butt joints*, *International Journal of Material Forming*, September, Volume 8, Issue 4, pp 591-599, 2015.
- [10] Citarella R., Carlone P., Sepe R., Lepore M., *DBEM crack propagation in friction stir welded aluminum joints*, *Advances in Engineering Software* 101, 50–59, 2016.
- [11] Citarella R., Cricri G., *Comparison of DBEM and FEM Crack Path Predictions in a notched Shaft under Torsion*, *Engineering Fracture Mechanics*, Vol.77, pp.1730-1749, 2010.
- [12] Citarella R., Lepore M., Shlyannikov V., Yarullin R., *Fatigue surface crack growth in cylindrical specimen under combined loading*, *Engineering Fracture Mechanics* 131, 439–453, 2014.
- [13] Citarella R., Buchholz F.-G., *Comparison of crack growth simulation by DBEM and FEM for SEN-specimens undergoing torsion or bending loading*, *Engineering Fracture Mechanics*, Vol. 75, pp. 489–509, 2008.
- [14] Citarella R., Cricri G., Lepore M., Perrella M., *DBEM and FEM Analysis of an Extrusion Press Fatigue Failure*. In: A. Öchsner, L.F.M. da Silva, H. Altenbach (eds.), *Materials with Complex Behaviour –Advanced Structured Materials*, 2010, Volume 3, Part 2, 181-191, Springer-Verlag, Berlin, Germany, 2010.
- [15] Citarella R., Giannella V., Lepore M.A., Fellingner J., Esposito R., *FEM-DBEM coupled procedure to analyse crack propagation in a baffle cooling pipe*, *Conference Proceedings of the 45° CONVEGNO NAZIONALE AIAS*, 7-10 September, Trieste, Italy, 2016.
- [16] Dassault Systèmes Simulia Corp., *Abaqus Analysis User's Manual*, Version 6.12.1, Providence, RI, USA, 2011.
- [17] BEASY, *BEASY V10r14 Documentation*. C.M. BEASY Ltd, 2011.
- [18] Rigby R.H., Aliabadi M.H., *Mixed-mode J-integral method for analysis of 3D fracture problems using BEM*. *Engng Anal Boundary Elem*, Vol. 11, pp. 239–56, 1993.
- [19] Rigby R.H., Aliabadi M.H., *Decomposition of the mixed-mode J-integral – revisited*, *Int J Solids Struct*, Vol. 35, No.17, pp. 2073–99, 1998.
- [20] Sih G.C., Cha B.C.K., *A fracture criterion for three-dimensional crack problems*, *J Engng Fract Mech*, Vol.6, pp. 699–732, 1974.